Integrated Optimization of Train Timetabling and Rolling Stock Circulation for Urban Rail Transit Under Tidal Passenger Flow

Yuxin Li, Changfeng Zhu, Yunqi Fu, Jie Wang, Linna Cheng, Rongjie Kuang

***Abstract*—Pronounced tidal passenger flow is manifested in the urban rail transit system during the peak period, presenting significant operational and scheduling challenges. An integrated optimization model that couples the train timetabling with rolling stock circulation under tidal passenger flow is developed, aiming to minimize passenger waiting time and train operation cost. Multiple real-world factors—including the safe-headway constraint, dwell-time calculation, and the feasibility of rolling stock connection—are fully considered in model development. To solve the nonlinear multi-objective optimization problem efficiently, an improved algorithm based on NSGA-II is proposed. A two-layer chromosome encoding scheme is adopted in the algorithm. The upper layer represents the train departure time, whereas the lower layer encodes the rolling stock connection. An adaptive penalty function is introduced to handle the constraints. A simulation study based on AFC data is conducted for Beijing Metro Line 6. Compared with the fixed-headway scheme, the optimized flexible scheme reduces operation cost by 18.2% and markedly shortens train connection time. Passenger waiting time increases by only about 9%. Thus, service quality is maintained and resource utilization is greatly improved by the optimized scheme. These findings verify the model's practicality and effectiveness under tidal passenger flow.**

***Index Terms*—urban rail transit, train timetabling, rolling stock circulation, integrated optimization**

I. INTRODUCTION

Metropolitan areas and urban clusters continue to expand. Urban functional zones now extend further outward, and the separation between residential and workplace locations has intensified. Consequently, the metro plays a core role in suburb-to-city-center commuting. Most existing lines still do not fully cover all functional zones. As a result, pronounced tidal passenger flow occurs on rail lines during the morning and evening peaks. To accommodate the temporal and spatial imbalances of passenger demand, a more flexible train operation scheme is urgently required. Train departure frequency and the number of rolling stock units can be dynamically adjusted. Joint optimization of the timetable and rolling stock circulation then enhances the match between line capacity and passenger demand.

Manuscript received April 30, 2025; revised August 19, 2025.

This work was supported in part by the National Natural Science Foundation of China (No.72161024) and "Double-First Class" Major Research Programs, Educational Department of Gansu Province (No.GSSYLXM-04).

Yuxin Li is a postgraduate student at School of Traffic and Transportation, Lanzhou Jiaotong University, Lanzhou 730070, China. (e-mail: 947046894@qq.com).

Changfeng Zhu is a professor at School of Traffic and Transportation, Lanzhou Jiaotong University, Lanzhou 730070, China. (Corresponding author, phone: +86 189 1989 1566, e-mail: cfzhu003@163.com).

Yunqi Fu is a doctoral candidate at School of Traffic and Transportation, Lanzhou Jiaotong University, Lanzhou 730070, China. (e-mail: 13240002@stu.lzjtu.edu.cn).

Jie Wang is a doctoral candidate at School of Traffic and Transportation, Lanzhou Jiaotong University, Lanzhou 730070, China. (e-mail: 1009696615@qq.com).

Linna Cheng is a doctoral candidate at School of Traffic and Transportation, Lanzhou Jiaotong University, Lanzhou 730070, China. (e-mail: chengjj@163.com).

Rongjie Kuang is a doctoral candidate at School of Traffic and Transportation, Lanzhou Jiaotong University, Lanzhou 730070, China. (e-mail: kuangrj@126.com).

A. Literature review

A.1. Train Timetabling

Early research on train timetabling optimization focused mainly on improving operational stability and robustness. Sparling et al. [1] extended the periodic-event scheduling problem (PESP) into a variable-period optimization framework. The framework minimizes the cycle length and thereby enhances network stability and robustness. Högdahl et al. [2] proposed a hybrid approach that combines microscopic simulation with optimization. By using simulation data to predict train delays, the method improves the train timetabling robustness and punctuality. Under uncertain passenger demand and transfer behavior, Wang et al. [3] applied a mixed strategy that uses both long and short train formations. They embedded this strategy in a multi-agent simulation, an ALNS heuristic and the Gurobi solver, which increases the train timetabling adaptability and robustness.

The growing emphasis on energy saving and emission reduction has shifted timetable optimization toward improving energy-use efficiency. Su et al. [4] proposed an "integrated timetable" framework that couples inter-station running-time allocation with speed-profile control in a two-layer formulation. They demonstrated its applicability to automated-train operation systems. Li et al. [5] integrated speed profile and train timetabling optimization with the objective of maximizing regenerative energy. Feng et al. [6] examined both single-train and multi-train settings. They proposed a hierarchical optimization strategy that delivers system-wide energy savings, although potential delay perturbations in real operation were not considered. Feng et al. [7] focused on train energy consumption. They introduced a braking-energy recovery mechanism into timetable design and achieved coordinated optimization of energy efficiency and passenger travel time.

In recent years, passenger demand orientation has become an increasingly important factor in train timetabling optimization. To address dynamic passenger demand, Niu et al. [8] built a binary-integer programming model for timetable optimization. By modelling passenger queuing and boarding behavior precisely, the model effectively alleviates boarding congestion under oversaturated flow. Ran et al. [9] targeted tidal-flow characteristics. They constructed a bi-objective timetable-optimization model that balances energy saving with passenger time saving. Zhang et al. [10] analyzed how differences in passenger load affect operating energy consumption. They sought Pareto-optimal solutions that reconcile energy use with running time. Although the above studies have improved operating efficiency, reduced energy consumption and enhanced passenger experience, they seldom examine how rolling stock circulation influences the overall operation plan. This omission can lead to uneven capacity allocation and higher operation costs. Consequently, integrated mechanisms that couple train timetabling optimization with rolling stock circulation must be explored to achieve comprehensive improvements in operational efficiency and resource utilization.

A.2. Rolling stock circulation

Early studies on rolling stock circulation focused on model formulation and algorithm design. Using the Dutch Noord–Oost line as a case study, Fioole et al. [11] developed a circulation plan that accommodates train coupling and uncoupling. They solved the train-composition and routing problem with a mixed-integer linear program (MILP), laying a mathematical foundation for rolling-stock circulation. Under a fixed-depot assumption, Frelin et al. [12] examined routing optimization for several task-allocation schemes and built separate models for linear, symmetric, and asymmetric assignments. Inspired by the vehicle-routing problem, Szeto et al. [13] used an artificial bee colony algorithm to handle capacity-constrained scheduling. The study demonstrates the potential of heuristic algorithms in complex rolling stock circulation. Mahmoudi et al. [14] employed a space–time state network and dynamic programming to obtain exact solutions for pickup-and-delivery tasks with time windows. Their method enhances synchronized vehicle routing and timetabling in time-dependent networks.

As models and algorithms matured, researchers introduced visualization to improve structural representation and controllability. Zheng et al. [15] abstracted train states into a rolling stock connection graph and solved it with a MILP. He et al. [16] formulated the Urban Transit Rolling-Stock Assignment Problem (UTRSAP) using column generation and a large neighborhood search algorithm. Driven by intelligent-dispatching needs, recent work has moved toward real-time optimization and adaptability to flexible train composition. Wang et al. [17] proposed a convex optimization model that integrates passenger demand, energy consumption, and travel time. The model moves real-time rolling-stock circulation closer to practical use. To manage demand uncertainty, Cacchiani et al. [18] embedded disturbance tolerances in their model. This enhancement improves schedule adaptability, service level, and capacity utilization. Zhou et al. [19] addressed the dynamism, imbalance, and randomness of passenger demand by formulating a two-stage stochastic program. The model couples flexible train compositions with a robust passenger-flow control strategy. Zhu et al. [20] compared coupled or uncoupled trains with fixed compositions. They proposed a “shadow-train” connection method for coupled and uncoupled train service.

Substantial progress has been achieved in model formulation, algorithm design, and dispatch responsiveness for rolling-stock circulation. Nevertheless, most studies assume a fixed train timetabling and seldom consider its coupling with rolling stock circulation, which limits the flexibility required in practice.

A.3. Integrated optimization of train timetabling and rolling stock circulation

In recent years the research focus has shifted to integrated optimization of train timetabling and rolling stock circulation. The goal is to harmonize resource allocation with passenger service quality. The traditional sequential approach optimizes the timetable and rolling-stock circulation independently, which causes decoupling. To resolve this issue, Wang et al. [21] proposed a two-stage framework. Stage 1 generates a demand-oriented timetable using a mixed-integer nonlinear program (MINLP). Stage 2 then refines this timetable with a mixed-integer linear program (MILP) to reduce the number of required trainsets. Building on this idea, Yao et al. [22] presented an integrated model. The linearized MILP formulation achieves high rolling stock utilization and service quality. Zhao et al. [23] observed that sequential optimization struggles to reconcile passenger experience with operating cost. They therefore unified running time, dwell time, and coupling–decoupling operations in a single model. Logical and piecewise-linearization techniques converted the resulting MINLP into a MILP, which greatly improved computational efficiency.

As tidal flow characteristics intensify, dynamic passenger demand has become a crucial component of integrated optimization models. On a line with pronounced tidal flows, Liu et al. [24] combined train coupling–uncoupling strategies with platform-flow control. They dynamically adjusted train headways and on-board capacity constraints. This approach deeply integrates the timetable with the circulation plan. A Lagrangian-relaxation heuristic solves the peak-period dispatching problem. Zhou et al. [25] incorporated passenger-flow control and used a tabu-search algorithm with the CPLEX solver to jointly optimize the timetable and rolling stock circulation. Yuan et al. [26] studied Beijing Metro Line 6 and introduced a short-turn strategy. They formulated a multi-objective MINLP and coupled a genetic algorithm with a commercial solver. The resulting plan integrates the timetable with rolling stock circulation and reduces average passenger waiting time.

B. Research gap

Existing studies consider integrated optimization under unbalanced demand. However, they often reduce multi-objective problems to single-objective problems through simplistic aggregation by using weighting coefficients. This simplification limits the diversity of trade-offs and solution possibilities. Consequently, the resulting models cannot fully capture the complex multidimensional trade-off between service quality and operational cost.

C. Contributions

To overcome these limitations, a multi-objective mixed-integer nonlinear programming (MINLP) model is formulated to simultaneously minimize passenger waiting time and operation cost, subject to headway, dwell-time, depot, and rolling stock connection constraints. The model is based on a rolling-stock connection network and explicitly captures the coupling between train timetabling and rolling stock circulation under tidal passenger flow conditions. A hybrid-encoding NSGA-II algorithm is developed to solve this model. The feasibility and effectiveness of the proposed approach are demonstrated through a case study on Beijing Metro Line 6.

II. Problem Statements

A. System description

Consider a metro line shown in Fig. 1. The line exhibits tidal passenger flow pattern and comprises s stations, whose set is denoted by $S=\{\bar{J},\underline{J},D\}$. Stations 1 and s serve as turn-back terminals. Within the study horizon $T=\{t_0,t_1,...,t_n\}$, the set of train services is denoted by $I=\{\bar{I},\underline{I},K\}$, and the set of rolling stock is denoted by $R=\{r_o|r_o=1,2,...,m\}$.

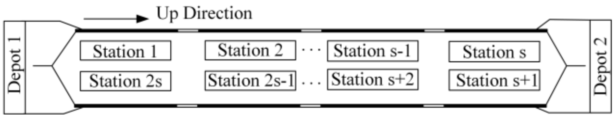

Fig. 1. The subway line layout

A passenger-demand-oriented train operation plan must simultaneously consider train arrival time, departure pattern, and rolling stock circulation. Train timetabling and rolling stock circulation are tightly interdependent: the departure frequency and the number of scheduled services determine how many trainsets are required, whereas the circulation plan constrains the timetabling. Under pronounced spatiotemporal heterogeneity of passenger demand, integrated optimization must achieve three objectives. First, it must closely match dynamically changing demand. Second, it must ensure a unique and feasible rolling stock succession for each service *i*. Third, it must prevent conflicts between revenue operations on the main line and depot movements.

B. Rolling stock connection network construction

Define the rolling stock connection graph $G=(V,E)$ as shown in Fig. 2, where $V=V_1\cup V_2$. $V_1=\{v_1^d|v_1^d=1,2,...,n\}$ is the set of depot nodes and $V_2=\{v_2^i|v_2^i=1,2,...,n\}$ is the set of train-service nodes. Each train-service node is annotated with its origin station S_i^d, terminal station S_i^a, departure time t_i^d, and arrival time t_i^a. The edge set is denoted by $E=\{e|e=(v_2^i,v_2^{i'}),(v_1^d,v_2^i)\}$. An edge *e* is created only if a feasible connection exists between its incident nodes v_1^d and v_2^i. Each connection edge *e* carries a weight $c_{i,i'}$, defined as the time interval between the completion of service *i* and the start of service *i′*. By constructing this rolling stock connection graph, train dispatching status and rolling stock connection relationships are comprehensively displayed.

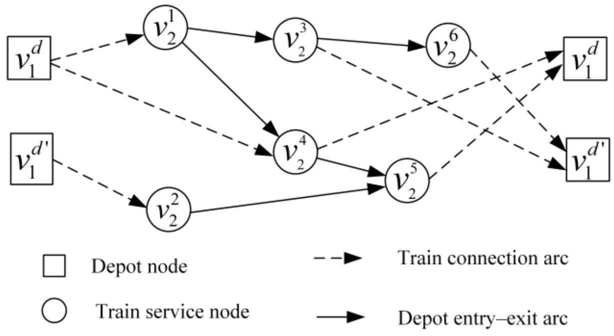

Fig. 2. Rolling stock connection graph

C. Assumptions

For the purpose of modeling the problem under study, the following assumptions are introduced:

Assumption 1. Passengers follow an alight-before-board rule, and the passenger arrival rate is derived from AFC data.

Assumption 2. Train operation is based on the all-station-stop scheme, and the section running time is pre-given.

Assumption 3. Train overtaking is not permitted on the line.

D. Notation

The sets, parameters, and indicators of the optimization model are listed in Table I, and the decision variables are shown in Table II.

TABLE I
SETS, PARAMETERS AND INDICATORS FOR THE OPTIMIZATION

Notations	Definition
S	Set of stations, $S=\{\bar{J},\underline{J},D\}$;
$\bar{J}$	Set of stations in the up direction, $\bar{J}=\{1,2,\ ...,s\}$;
$\underline{J}$	Set of stations in the down direction, $\underline{J}=\{s+1,...,2s-1,2s\}$;
D	Set of depots, $D=\{1,2\}$;
j,d	Index of stations, $j,d\in S$;
I	Set of the train services, $I=\{\bar{I},\underline{I},K\}$;
$\bar{I}$	Set of train services in the up direction, $\bar{I}=\{1,2,...,i\}$;
$\underline{I}$	Set of train services in the down direction, $\underline{I}=\{1,2,...,i'\}$;
K	Set of the train services which out of/into the depots, $K=\{1,2,...,k\}$;
i,k	Index of the train services, $i,k\in I$;
T	Set of operational time, $T=\{t_0,t_1,...,t_n\}$;
τ	Set of time interval, $\tau=t_n-t_{n-1}$;
$t_{i,j}^{\text{run}}$	The time for service *i* running between station *j*-1 and *j*;
$t_{p,j}^{\text{up}}$	The time for passenger to board at station *j*;
$t_{p,j}^{\text{down}}$	The time for passenger to alight at station *j*;
$t_{\text{o}}^{\text{door}}$	The time for the rolling stock to open the door;
$t_{\text{c}}^{\text{door}}$	The time for the rolling stock to close the door;
t_{brake}	The time for the rolling stock to brake;
$t_{i,\min}^{\text{w}}$	the minimum time for service *i* to dwell;
$t_{i,\max}^{\text{w}}$	the maximum time for service *i* to dwell;

$t_{i,j}^{\min}$	the minimum headways for two consecutive services;
$t_{i,j}^{\max}$	the maximum headways for two consecutive services;
$t_{\text{turn}}^{\min}$	the minimum time standards for the rolling stock to turn around from the station s to s+1/2s to 1;
$t_{\text{turn}}^{\max}$	the maximum time standards for the rolling stock to turn around from the station s to s+1/2s to 1;
t_{cleaning}	The time for cleaning the conveys;
c_1	Operation cost for one rolling stock to run;
θ	Operation cost for one rolling stock to turnaround per minute;
$C_{\max}$	Maximum capacity of one rolling stock;
M	A large positive number;
N_d	The capacity of the depots;
$N_{j,t}^{\mathrm{w}}$	The number of passengers waiting the train.

TABLE II
DECISION VARIABLES FOR THE OPTIMIZATION MODEL

Variables	Definition
$t_{i,j}^{\mathrm{a}}$	continuous variable, time for service i to arrive at station j;
$t_{i,j}^{\mathrm{d}}$	continuous variable, time for service i to departure from station j;
$\gamma_i^{r_o,d}$	Binary variable, if rolling stock r_o takes service i, $\gamma_i^{r_o,m}=1$, otherwise $\gamma_i^{r_o,m}=0$;
$\zeta_{i,i'}^{r_o,d}$	Binary variable, if rolling stock r_o continues from service i to i', $\zeta_{i,i'}^{r_o,m}=1$, otherwise $\zeta_{i,i'}^{r_o,m}=0$.

III. MATHEMATICAL MODEL

A. Constraint conditions

A.1. Timetable constraints

The arrival and departure time of each train at each station are determined by the section running time and the station dwell time. Accordingly, the arrival and departure time of each train service i at station j are expressed as:

$$t_{i,j}^{\mathrm{a}}=t_{i,j-1}^{\mathrm{d}}+t_{i,j}^{\mathrm{run}},\ \ \forall i\in\overline{I},j,\ \ j-1\in\overline{J}\,\text{or}\,\forall i\in\underline{I},j\in\underline{J} \tag{1}$$

$$t_{i,j}^{\mathrm{d}}=t_{i,j}^{\mathrm{a}}+t_{i,j}^{\mathrm{w}},\ \ \forall i\in\overline{I},j,\ \ j-1\in\overline{J}\,\text{or}\,\forall i\in\underline{I},j\in\underline{J} \tag{2}$$

The station dwell time consists mainly of three components: the door opening-closing time, the average boarding-and-alighting time of platform passengers, and the braking time. The dwell time is given by the following formula:

$$\begin{gathered}t_{i,j}^{\mathrm{w}}=t_{p,j}^{\mathrm{up}}+t_{p,j}^{\mathrm{down}}+t_{o}^{\mathrm{door}}+t_{c}^{\mathrm{door}}+t_{\mathrm{brake}},\\ \forall i\in\overline{I},j\in\overline{J}\,\text{or}\ \forall i\in\underline{I},j\in\underline{J}\end{gathered} \tag{3}$$

To ensure both operation efficiency and safety, the dwell time must also satisfy the following constraint:

$$t_{i,\min}^{\mathrm{w}}\le t_{i,j}^{\mathrm{w}}\le t_{i,\max}^{\mathrm{w}},\forall i\in\overline{I},j\in\overline{J}\,\text{or}\,\forall i\in\underline{I},j\in\underline{J} \tag{4}$$

The train headway is a key indicator of service quality in urban railway transit. it directly affects both line capacity and passenger waiting time. The headway between two successive trains is defined as following:

$$\begin{gathered}t_{i,j}=t_{i,j-1}+t_{i+1,j-1}^{w}-t_{i,j-1}^{w},\\ \forall i,i+1\in\overline{I},j,j-1\in\overline{J}\ \text{or}\ \forall i,i+1\in\underline{I},j,j-1\in\underline{J}\end{gathered} \tag{5}$$

To guarantee operation safety service efficiency, the headway between a two successive trains must satisfy the following:

$$\text{t}\qquad t_{i,j}^{\min}\le t_{i,j}\le t_{i,j}^{\max},\forall i\in\overline{I},j\in\overline{J}\,\text{or}\,\forall i\in\underline{I},j\in\underline{J} \tag{6}$$

A.2. Rolling stock constraints

Each rolling stock unit r_o can only serve at most one train service at any time:

$$\sum_{d\in D}\sum_{r_o\in R}\gamma_i^{r_o,d}=1,\ \ \forall i\in\overline{I},i'\in\underline{I}\ \text{or}\ \forall i\in\underline{I},i'\in\overline{I} \tag{7}$$

Each rolling stock r_o must have exactly one predecessor and one successor, ensuring a complete and error-free connection order:

$$\sum_{d\in D}\sum_{r_o\in R}\sum_{i'\in I}\zeta_{i',i}^{r_o,d}-\sum_{d\in D}\sum_{r_o\in R}\sum_{i'\in I}\zeta_{i,i'}^{r_o,d}=0,\ \ \forall i\in\overline{I}\,\text{or}\,\forall i\in\underline{I} \tag{8}$$

At a depot-departure node, rolling stock can flow only outward; at a depot-arrival node, it can flow only inward:

$$\sum_{d\in D}\sum_{r_o\in R}\sum_{i\in I}\zeta_{k,i}^{r_o,d}=1,\ \ \forall k\in K \tag{9}$$

$$\sum_{d\in D}\sum_{r_o\in R}\sum_{i\in I}\zeta_{i,k}^{r_o,d}=1,\ \ \forall k\in K \tag{10}$$

The depot capacity must be sufficient to accommodate the number of trainsets required for the daily service:

$$\sum_{r_o\in R}\sum_{k\in K}\sum_{i\in I}\zeta_{k,i}^{r_o,d}\le N_d,\ \ \forall d\in D \tag{11}$$

For operational flexibility, a trainset may depart from one depot and return to another, but each depot's departures must equal its returns:

$$\sum_{r_o\in R}\sum_{k\in K}\zeta_{k,i}^{r_o,d}=\sum_{r_o\in R}\sum_{k\in K}\zeta_{i,k}^{r_o,d},\ \ \forall i\in I,d\in D \tag{12}$$

After completing service i, a rolling stock may proceed to service i+1 only if the connection-capability criterion and the turnaround-time requirement are both satisfied:

$$\begin{gathered}t_{i',j'}^{\mathrm{a}}-t_{i,j}^{\mathrm{d}}\ge t_{\text{turn}}^{\min}-M(1-\zeta_{i',i}^{r_o,d}),\\ \forall i\in\overline{I},j=1,i'\in\underline{I},j'=2s\ \text{or}\ i\in\underline{I},j=s+1,i'\in\overline{I},j'=s\end{gathered} \tag{13}$$

$$\begin{gathered}t_{i',j'}^{\mathrm{a}}-t_{i,j}^{\mathrm{d}}\le t_{\text{turn}}^{\max}+M(1-\zeta_{i',i}^{r_o,d}),\\ \forall i\in\overline{I},j=1,i'\in\underline{I},j'=2s\ \text{or}\ i\in\underline{I},j=s+1,i'\in\overline{I},j'=s\end{gathered} \tag{14}$$

$$t_{i',j'}^{\mathrm{a}}-t_{i,j}^{\mathrm{d}}=c_{i,i'}=t_{\text{turn}}+t_{\text{cleaning}} \tag{15}$$

B. Objective function

B.1. Passenger waiting time

The average passenger waiting time is generally assumed to be one-half of the train departure headway; hence, optimizing passenger waiting time is tantamount to optimizing the train departure headway. Passenger waiting time is expressed as:

$$\min Z_1=\frac{1}{2}\sum_{i=1}^{I}\sum_{j=1}^{S}\sum_{t=t_1}^{t_n}N_{j,t}^{\mathrm{w}}t_{i,j} \tag{16}$$

B.2. Train operation cost

Operation cost comprises two components: the fixed cost of each trainset and the cost associated with succession time. These terms capture, respectively, the number of trainsets in service and the quality of rolling stock connection. The total operating cost is given by:

$$\min Z_2 = c_1 \sum_{d\in D}\sum_{r_o\in R}\sum_{k,i\in I} \xi_{k,i}^{r_o,d} + \theta \sum_{i\in I}\sum_{i'\in I} c_{i',i}\gamma_{i',i} \tag{17}$$

IV. ALGORITHM DESIGN

Uder the tidal flow condition, train timetabling and rolling stock circulation are tightly coupled. Even small adjustments to departure and arrival time can disrupt connection feasibility and degrade resource utilization. Conversely, deployment limits on rolling stock constrain timetable feasibility. The resulting optimization model contains coupled integer and continuous variables and nonlinear objectives under complex constraints, so conventional mathematical-programming methods are unsuitable. Therefore, the model is solved using the NSGA-II algorithm.

A. Chromosome encoding design

Timetabling variables are continuous, and headways must satisfy safety constraints. Rolling stock circulation, by contrast, is discrete and requires a unique, feasible connection. Therefore, a two-layer hybrid chromosome encoding scheme is adopted.

The upper layer uses real-valued encoding $y_1 = \{t_{1,1}^{\mathrm{a}}, t_{1,1}^{\mathrm{d}}, \ldots, t_{I,S}^{\mathrm{a}}, t_{I,S}^{\mathrm{d}}\}$ to represent train departure times, whereas the lower layer uses integer encoding $y_2 = \left\{\zeta_{i,i'}^{r_o,d}, \gamma_i^{r_o,d}\right\}$ to represent rolling stock connection. This design facilitates precise headway control and provides an intuitive representation of rolling stock connection.

B. Construction of the fitness evaluation

During algorithm execution, some individuals $Z = (Z_1, Z_2)$ violate hard constraints such as insufficient headway or depot overcapacity. The fitness evaluation therefore incorporates a penalty mechanism $\tilde{Z}_i(\mathbf{g}) = Z_i(\mathbf{g}) + \lambda_i \cdot P(\mathbf{g})$. The objective-function values of infeasible individuals are downgraded, guiding the population toward the feasible solution space.

C. Evolutionary strategy and constraint handling

During the evolutionary process, the following procedure is implemented within the NSGA-II framework :

Step 1—Population initialization: an initial population $\mathcal{G}^0$ is generated that satisfies the basic constraints.

Step 2—Non-dominated sorting: each individual in the population is rapidly ranked according to $(\tilde{Z}_1, \tilde{Z}_2)$ and assigned to a non-dominated front $F1, F2, \ldots$.

Step 3—Crowding-distance calculation: the crowding distance $\mathrm{CD}(\mathbf{g}_k)$ is computed for every individual within each non-dominated front.

Step 4—Selection: tournament selection based on rank and crowding distance is applied to generate the parent set $\mathcal{G}^p$.

Step 5—Crossover and mutation: simulated binary crossover and Gaussian-perturbation mutation are performed on t^{d} whereas single-point crossover and swap mutation are applied to $\gamma_i^{r_o,d}$、$\zeta_{i,i'}^{r_o,d}$.

Step 6—Repair mechanism: if a new individual $\mathbf{g}'$ violates the train headway or the connection rule, local reordering or departure time adjustment is carried out.

Step 7—Elitism: the parent and offspring populations are merged, and the best N individuals are selected to form the next generation $\mathcal{G}^{t+1}$.

D. Evolutionary convergence criteria and solution out-put

In each iteration, the algorithm merges the parent and offspring populations and selects elite individuals jointly on the basis of non-dominated rank and crowding distance. The procedure terminates when either (i) the maximum number of generations $G_{\max}$ is reached or (ii) the variation in the Pareto set remains below the threshold ϵ for δ consecutive generations; the final output is the non-dominated solution set $\mathcal{P}^* = \{\mathbf{g}_1^*, \ldots, \mathbf{g}_K^*\}$. The overall flowchart of the algorithm is presented in Fig. 3.

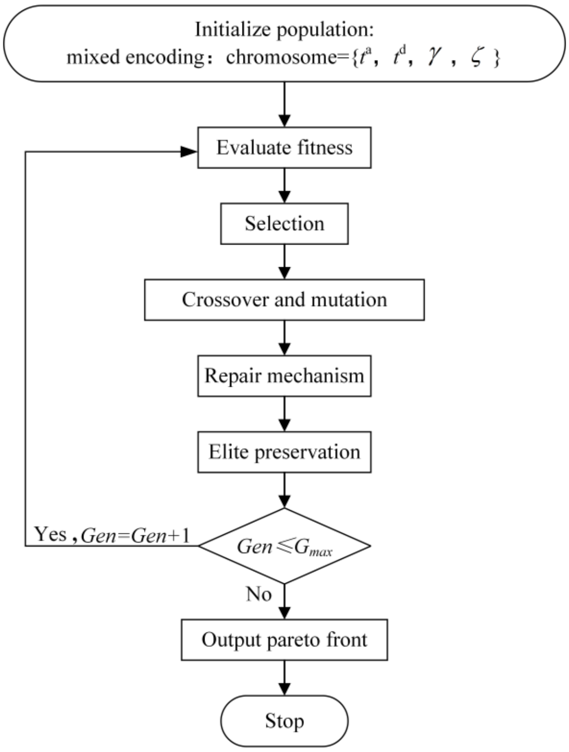

Fig. 3. The algorithm flow chart

V. NUMERICAL EXPERIMENTS

A. Case introduction

This study examines a bidirectional urban rail line with a total length of 28.38 km. Stabling yards and depots are located at the two terminals, and the line operates with fixed-consist train formations. The line comprises 20 stations in total, and both terminal stations serve as turn-back points. The analysis horizon is the morning period T=[6:00-10:00], with a time interval of $\tau = 10\,\mathrm{min}$. Parameter settings for the integrated timetabling and rolling stock optimization model are provided in Table III.

TABLE III
VALUE OF THE RELEVANT PARAMETERS

parameters	value	parameters	value
$t_{\text{o}}^{\text{door}}$	3s	$t_{i,j}^{\min}$	1.5min
$t_{\text{c}}^{\text{door}}$	3s	$t_{i,j}^{\max}$	15min
$t_{i,\min}^{\text{w}}$	20s	c_1	10000
$t_{i,\max}^{\text{w}}$	60s	θ	100
$t_{\text{turn}}^{\min}$	1.5min	$C_{\max}$	1860
$t_{\text{turn}}^{\max}$	10min		

Passenger arrival rates for each time interval are extracted from the AFC system for both the up and down directions. These rates are plotted in Fig. 4(a) and Fig. 4(b), respectively. Both directions exhibit pronounced morning peaks within the 6:00–10:00 horizon. The up-direction peak occurs earlier and is stronger, producing a single-peak profile. By contrast, the down-direction peak occurs later, has lower intensity, and lasts longer, showing several smaller sub-peaks. Overall, the line exhibits a clear tidal-flow pattern.

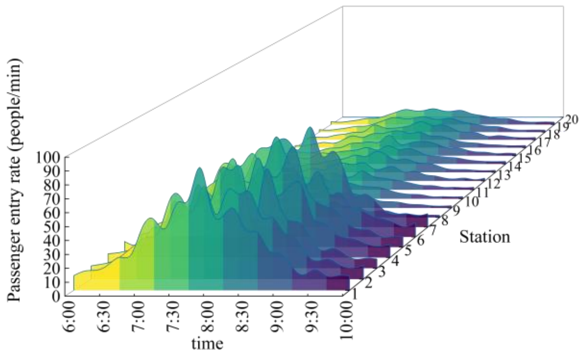

Fig. 4(a). The entry rate of passengers in the up direction

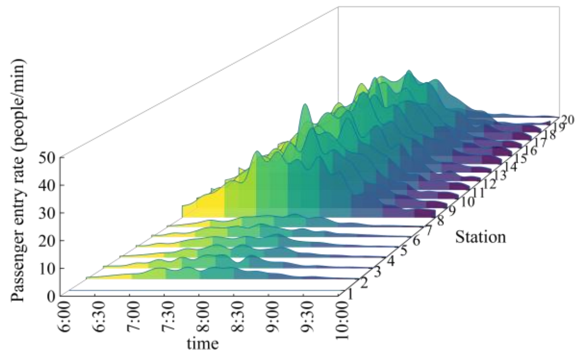

Fig. 4(b). The entry rate of passengers in the down direction

B. Computational results

The model is solved in a Python environment. To balance solution diversity with convergence speed—and to maintain reasonable runtime—the algorithm parameters are set as follows: $N_S = 300$, $N_g = 100$, $N_{cr} = 0.8$, $N_{mr} = 0.6$ .The HV iteration curve and Pareto frontier obtained under these settings are displayed in Fig. 5 and Fig. 6, respectively.

Fig. 5 shows that the HV curve rises steeply in the early generations, indicating that high-quality solutions are obtained quickly at the outset. The growth rate slows between generations 20 and 30, and a knee point appears around generations 30–40, after which the algorithm enters its late-convergence phase. By generations 80–100, the HV stabilizes at 0.95–0.96 and hardly increases further, indicating algorithm convergence.

The HV metric reflects the overall quality and spread of the solution set; however, the detailed optimization effect is best examined through the Pareto frontier. Fig. 6 demonstrates a clear trade-off between objectives: as Objective 1 increases, Objective 2 gradually decreases, confirming a marked conflict.

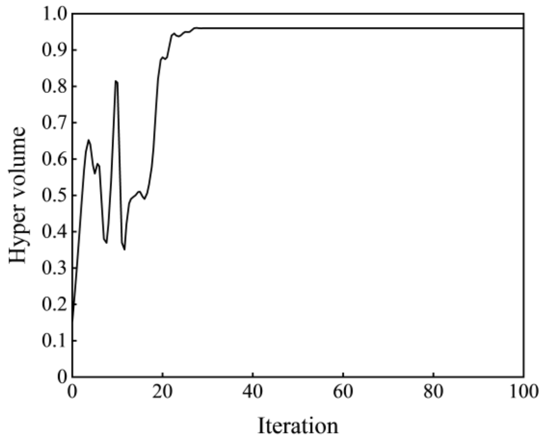

Fig. 5. The HV iteration curve

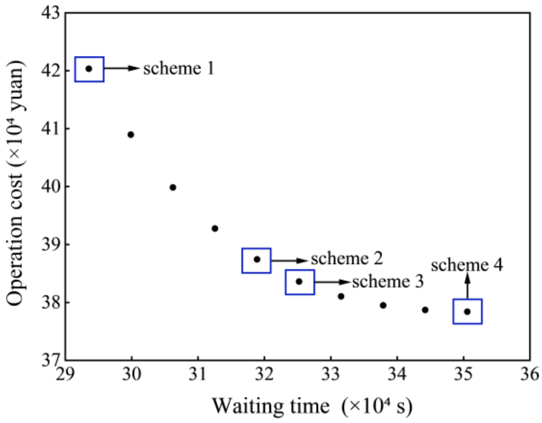

Fig. 6. The pareto front scheme

The Pareto solutions and their classifications are summarized in Table IV. Table IV reveals a pronounced trade-off between operating cost and passenger waiting time. As the operating cost decreases from 420339 in Scheme 1 to 378399 in Scheme 4, the total waiting time rises from 293537 min to 350566 min. Among the four schemes, Scheme 2 delivers the smallest increase in waiting time per unit of cost saved, marking the best marginal-benefit pivot. Beyond this point, further cost reductions lead to disproportionately large losses in service quality. Hence, Scheme 2 represents the optimal compromise on the multi-objective Pareto frontier and is the preferred choice when both economy and service quality matter. Scheme 1 and Scheme 4 represent the two extremes—"service-first" and "cost-first," respectively. Scheme 3 also lies on the frontier, but its marginal benefit is weaker than that of Scheme 2. Operators can therefore select among these Pareto solutions according to their strategic priorities.

From the Pareto frontier, Scheme 2 is selected as the best compromise between economy and service quality. Under this scheme, the total passenger waiting time Z_1 is 318883 min, and the operating cost Z_2 is 387425.

TABLE IV
PARETO FRONT SCHEME

Scheme	Waiting Time/min	Operation Cost	Classification
1	293537	420339	Service-level priority.
2	318883	387425	Best marginal benefit.
3	325219	383605	Moderate compromise.
4	350566	378399	Cost-priority.

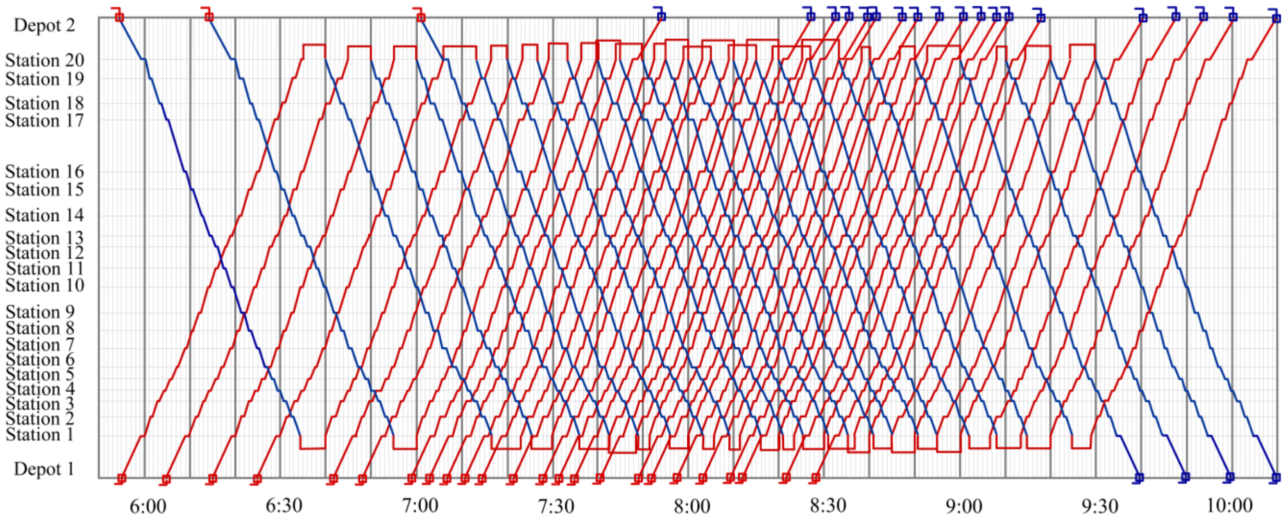

Fig. 7. The optimized train timetable

The optimized train timetable is presented in Fig. 7. Fig. 7 shows that 73 train services are scheduled within the horizon $T=[6:00,10:00]$: 47 train services in the up direction and 26 in the down direction. A total of 27 trainsets are deployed. The departure frequency first increases and then decreases as time progresses.

A statistical and time-series analysis is performed on the headway data in Fig. 8(a) and Fig. 8(b) for the 6:00-10:00 operation window.

The mean departure interval is 4.46 min in the up direction and 8.43 min in the down direction. Headways are aggregated in 15-min bins to reveal a typical tidal pattern.

In the up direction, the interval shortens rapidly after 6:00, reaches approximately 3 min during the 7:30-8:30 peak, and then rises to 5-7 min.

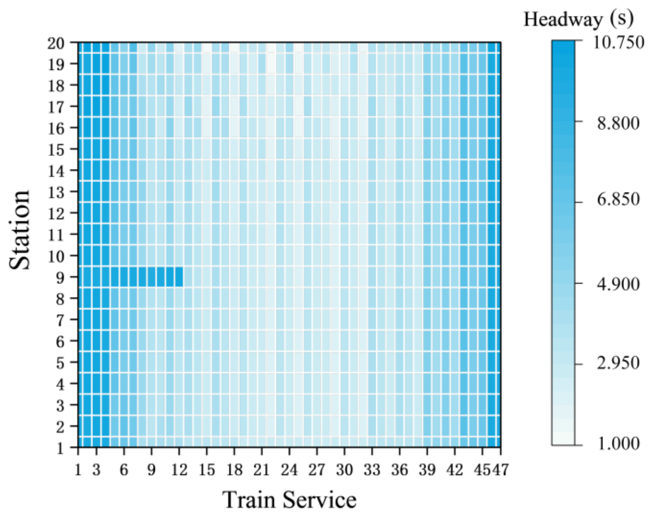

Fig. 8 (a) The departure interval of trains in the up direction

In the down direction, the interval initially decreases and then increases: it is roughly 20 min between 6:00 and 7:00, falls to about 5 min between 8:00 and 9:00, and widens to 13 min before 10:00.

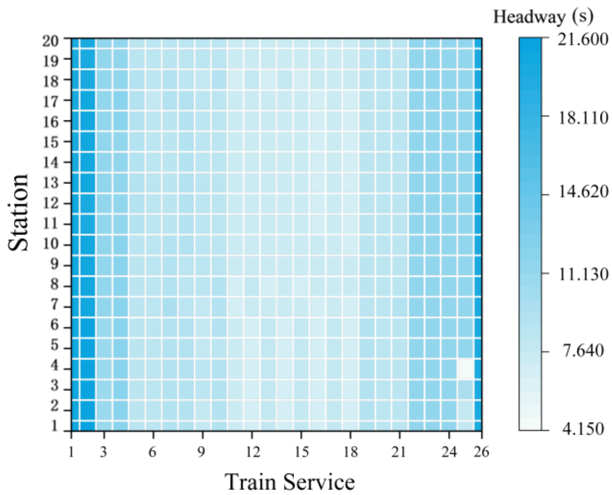

Fig. 8 (b) The departure interval of trains in the down direction

These results show that the optimized rolling stock plan adjusts headways to match asymmetric demand. However, some down-direction headways remain long; introducing flexible train compositions could further improve service quality.

C. Results analysis

C.1. Sensitivity analysis of population size

To evaluate how the population size N_S influences the convergence of NSGA-II in the integrated optimization of the timetabling and rolling stock circulation, a single-factor experiment is constructed based on the previous case.

All model parameters are fixed except N_S. Four values of N_S are tested: 200, 250, 300, 350. The evolution of HV metric under each setting is plotted in Fig. 9.

HV is highly sensitive to a population size of 350. With the population size of 350, the algorithm reaches 90% of its final HV by generation 7. In contrast, a population size of 200 requires at least 12 generations to achieve the same level. A larger initial population thus enhances diversity, accelerating the global search.

All curves eventually converge and cluster at an HV of approximately 0.86; the final gap among settings narrows to 0.01-0.02. Thus, NSGA-II demonstrates strong robustness to population size once it enters this "low-sensitivity" phase.

Increasing the population size N_S from 300 to 350 yields only about a 1% gain in HV, yet the computation time nearly triples. Such a marginal benefit does not offset the substantial increase in computational cost.

Balancing convergence speed, solution quality, and runtime, a population size of 300 is the best compromise for the present model. With this setting, the algorithm attains 95% of its final HV within roughly ten generations.

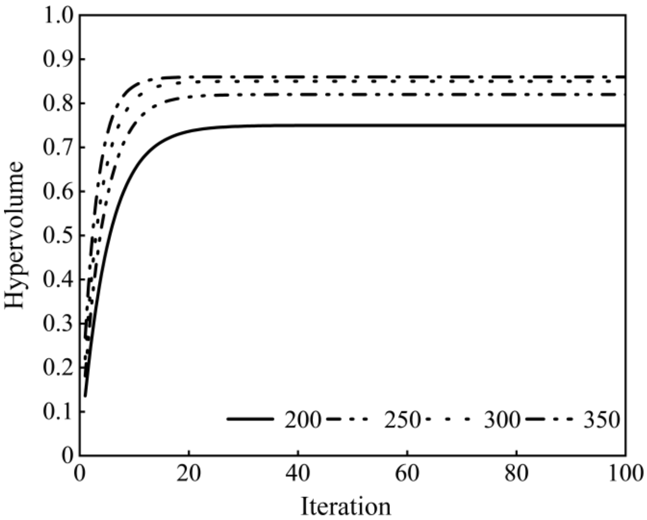

Fig. 9 Convergence analysis plot

C.2. Comparative analysis of different headway schemes

To evaluate how different headway settings affect the performance of the timetable and rolling stock plan, three schemes are compared: a 5-min uniform headway, a 15-min uniform headway, and the optimized flexible-headway scheme. Evaluation indicators for the three schemes are listed in Table V.

Table V shows that although the 15-min uniform scheme consumes the fewest resources, it fails to meet actual passenger demand and is therefore infeasible in practice. Compared with the 5-min uniform scheme, the flexible-headway scheme increases passenger waiting time by only about 11.7% while reducing operating cost by approximately 21%, demonstrating superior cost-control capability.

Regarding fleet size, the flexible-headway scheme requires approximately 18.2% fewer trainsets than the 5-min uniform scheme, thus saving resources while still satisfying passenger demand. The unequal-headway scheme also provides a more flexible succession plan, reducing train succession time by about 50% relative to the 5-min uniform scheme.

In summary, the unequal-headway scheme effectively combines the advantages of passenger service quality and economic efficiency. It outperforms the uniform-headway schemes in resource conservation, cost control, demand matching, and balanced rolling-stock utilization, making it better suited to operational conditions under tidal passenger flow.

C.3. Average load factor comparison

To evaluate how different departure-headway schemes affect rolling stock utilization, we compared the average train load factors under the balanced schemes (5 min, 15 min) and the unequal-headway scheme. The average load factors for the up and down directions are given in Fig. 10(a) and Fig. 10(b), respectively.

Fig. 10(a) shows that the 15 min uniform scheme produces the highest overall average load factor in the up direction; most trains exceed the full-load threshold, indicating insufficient capacity, serious crowding, and poor service quality. The 5 min uniform scheme keeps the load factor roughly within 0.85-1.2, and the cars remain crowded. The flexible headway scheme is more balanced, demonstrating a good match between capacity and demand and a more reasonable allocation of train capacity.

In the down direction, the 15 min uniform scheme yields intermediate load factors of 0.4-0.8; the value is high in the early and middle portions of the period and then falls, showing large fluctuations and moderate stability. The 5 min uniform scheme keeps the load factor low, always between 0.1 and 0.6, indicating obvious excess capacity and low resource utilization. The flexible headway scheme consistently performs best: its load factor stays steadily at 0.7-0.9, and its curve is markedly more stable than those of the other schemes, better matching actual demand and providing higher resource-utilization efficiency and enhanced service stability.

Thus, the optimized unequal-headway scheme offers clear advantages in both directions. It effectively matches tidal-flow demand, maintains passenger service quality, and significantly improves overall resource utilization and operational stability.

TABLE V
PERFORMANCE COMPARISON UNDER DIFFERENT HEADWAY SCHEMES

Scheme	Headway	Connection time/min	Waiting time/min	Operating cost	Rolling stock
Uniform headway	5 min	464	297811	495870	33
Uniform headway	15 min	175	887388	166550	12
Flexible headway	Variable	252	325219	383605	27

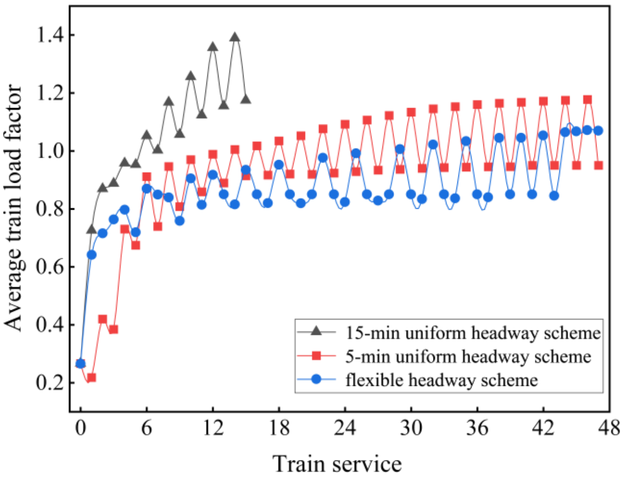

Fig. 10 (a) The average train load factor in the up direction

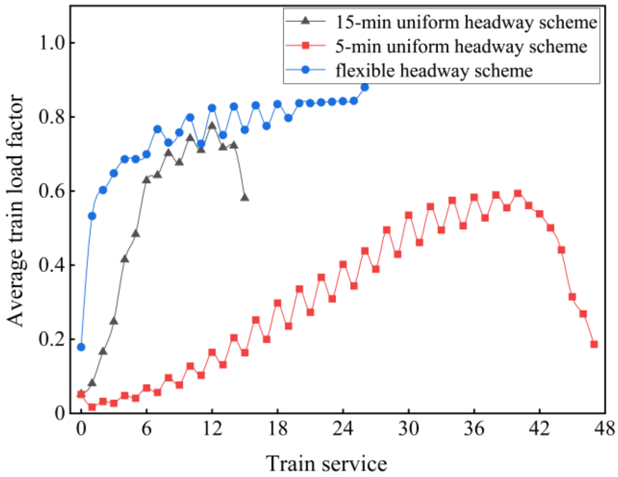

Fig. 10 (b) The average train load factor in the down direction

VI. Conclusion And Discussion

(1) **Development of a space-time tidal flow multi-objective model.** Focusing on the spatiotemporal distribution of tidal passenger flow, this study adopts a rolling stock succession graph to describe train-node attributes and edge constraints. A mixed integer multi-objective nonlinear program is formulated to minimize passenger waiting time and train operation cost. The model integrates train arrival–departure time, dwell time, headway limits, and rolling stock constraints, thereby capturing the coupling between train operation and resource scheduling and providing a theoretical basis for efficient metro operation.

(2) **Design and implementation of an enhanced NSGA-II algorithm.** An empirical analysis is carried out with real metro data. The model is solved by an NSGA-II-based evolutionary algorithm with a two-layer chromosome. Simulation results show that the optimized unequal-headway scheme outperforms the 5-min uniform scheme and 15-min uniform scheme. Passenger waiting time falls by nearly 21% while operation cost rises by only about 11.7%. Average load factors become more balanced, and carrying efficiency improves in both directions.

(3) **Population size sensitivity analysis and optimal setting.** A sensitivity test on population sizes 200, 250, 300, 350 indicates a "high-sensitivity" phase in the first 20 generations, during which larger populations raise the HV value faster. After generation 50, all curves converge at an HV of about 0.86, with final differences below 0.02. Considering convergence speed, solution quality, and runtime, a population of 300 reaches 95% of the final HV within about ten generations and offers the best cost-benefit balance.

(4) **Application prospects.** The present model assumes fixed train consists and does not fully account for flexible coupling-uncoupling strategies such as "add cars in peaks, cut cars in off-peaks." Future work should treat consist size as a decision variable, allowing dynamic adjustment by time period and direction. This extension is expected to raise capacity utilization, accommodate demand fluctuations, and further improve service quality.

References

[1] D. Sparing and R. M. P. Goverde, "A cycle time optimization model for generating stable periodic railway timetables," *Transportation Research Part B: Methodological*, vol. 98, pp. 198–223, 2017.

[2] J. Högdahl and M. Bohlin, "A combined simulation-optimization approach for robust timetabling on main railway lines," *Transportation Science*, vol. 57, no. 1, pp. 52–81, 2023.

[3] F. Wang, P. Wang, Z. Zhu, R. Xu, H. Pan, and N. Bešinović, "Robust optimization of train timetables with short-length and full-length services considering uncertain passenger volume and service choice behavior," *Transportation Research Part C: Emerging Technologies*, vol. 169, pp. 104855, 2024

[4] S. Su, X. Li, T. Tang, and Z. Gao, "A subway train timetable optimization approach based on energy-efficient operation strategy," *IEEE Transactions on Intelligent Transportation Systems*, vol. 14, no. 2, pp. 883–893, 2013.

[5] X. Li and H. K. Lo, "An energy-efficient scheduling and speed control approach for metro rail operations," *Transportation Research Part B: Methodological*, vol. 64, pp. 73–89, 2014.

[6] Y. Feng, S. Chen, X. Ran, Y. Bai, and W. Jia, "Energy-efficient train operation optimization in urban rail transit considering regenerative braking energy," *Journal of the China Railway Society*, vol. 40, no. 2, pp. 15–22, 2018.

[7] J. Feng, X. Li, J. Shi, and Y. Shi, "Joint optimization of metro train timetable and stopping plan for the first service period: An integrated energy-efficient and time-saving model," *International Journal of Transportation Science and Technology*, vol. 13, no. 2, pp. 189–207, 2024.

[8] H. Niu and X. Zhou, "Optimizing urban rail timetable under time-dependent demand and oversaturated conditions," *Transportation Research Part C: Emerging Technologies*, vol. 36, pp. 212–230, 2013.

[9] X. Ran, S. Chen, Y. Bai, Y. Chen, Z. Chen, and C. Yang, "Energy-saving and passenger time-saving timetable optimization model for urban rail transit under tidal passenger flow," *China Railway Science*, vol. 43, no. 1, pp. 171–181, 2022.

[10] H. Zhang, F. Dou, Y. Wei, J. Liu, and Y. Ning, "Timetable optimization method considering net energy consumption and passenger load differences of trains," *Journal of Transportation Systems Engineering and Information Technology*, vol. 23, no. 2, pp. 208–216, 2023.

[11] P.-J. Fioole, L. Kroon, G. Maróti, and A. Schrijver, "A rolling stock circulation model for combining and splitting of passenger trains," *European Journal of Operational Research*, vol. 174, no. 2, pp. 1281–1297, 2006.

[12] R. Freling, A. P. M. Wagelmans, and J. M. P. Paixão, "Models and algorithms for single-depot vehicle scheduling," *Transportation Science*, vol. 35, no. 2, pp. 165–180, 2001.

[13] W. Y. Szeto, Y. Wu, and S. C. Ho, "An artificial bee colony algorithm for the capacitated vehicle routing problem," *European Journal of Operational Research,* vol. 215, no. 1, pp. 126–135, 2011.

[14] M. Mahmoudi and X. Zhou, "Finding optimal solutions for vehicle routing problem with pickup and delivery services with time windows: A dynamic programming approach based on state-space-time network representations," *Transportation Research Part B: Methodological*, vol. 89, pp. 19–42, 2016.

[15] L. Zheng, R. Song, Y. Xiao, and J. Liu, "Optimization method for rolling stock scheduling under network-based operation of urban rail transit," *China Railway Science*, vol. 35, no. 2, pp. 104–110, 2014.

[16] B. He, R. Song, S. He, and J. Li, "A hybrid column generation algorithm for urban rail transit rolling stock scheduling optimization model," *China Railway Science*, vol. 35, no. 1, pp. 122–129, 2014.

[17] Y. Wang, B. Ning, T. Tang, T. J. J. van den Boom, and B. De Schutter, "Efficient real-time train scheduling for urban rail transit systems using iterative convex programming," *IEEE Transactions on Intelligent Transportation Systems*, vol. 17, no. X, pp. 1–13, 2015. (pagination may vary due to online-first status)

[18] V. Cacchiani, J. Qi, and L. Yang, "Robust optimization models for integrated train stop planning and timetabling with passenger demand uncertainty," *Transportation Research Part B: Methodological*, vol. 136, pp. 1–29, 2020.

[19] H. Zhou, J. Qi, L. Yang, J. Shi, and C. Gong, "Joint optimization for rolling stock circulation plan based on flexible train composition mode and robust passenger flow control strategy on urban rail transit lines," *Control and Decision,* vol. 38, no. 9, pp. 2663–2671, 2023.

[20] C. Zhu, J. Jia, B. Ma, Y. Sun, J. Wang, and L. Cheng, "Research on optimization of rolling stock scheduling scheme for urban rail transit under reconnection marshalling," *Journal of Railway Science and Engineering, early access*, Apr. 8, 2024.

[21] Y. Wang, Z. Liao, T. Tang, and B. Ning, "Train scheduling and circulation planning in urban rail transit lines," *Control Engineering Practice*, vol. 61, pp. 112–123, 2017.

[22] Y. Yao, X. Zhu, L. Kang, and Z. Liao, "An integrated optimization model of train timetabling and rolling stock scheduling for an urban railway line," *Journal of Transportation Systems Engineering and Information Technology*, vol. 18, no. 1, pp. 200–206, 2018.

[23] Y. Zhao, D. Li, Y. Yin, and X. Zhao, "Integrated optimization of demand-driven timetable, train formation plan and rolling stock circulation with variable running times and dwell times," *Transportation Research Part E: Logistics and Transportation Review*, vol. 171, pp. 103035, 2023.

[24] R. Liu, S. Li, and L. Yang, "Collaborative optimization for metro train scheduling and train connections combined with passenger flow control strategy," *Omega,* vol. 99, pp. 102180, 2020.

[25] Y. Zhou, J. Qi, L. Yang, J. Shi, H. Pan, and Y. Gao, "Joint optimization of train timetabling and rolling stock circulation planning: A novel flexible train composition mode," *Transportation Research Part B: Methodological*, vol. 162, pp. 352–385, 2022.

[26] J. Yuan, Y. Gao, S. Li, P. Liu, and L. Yang, "Integrated optimization of train timetable, rolling stock assignment and short-turning strategy for a metro line," *European Journal of Operational Research*, vol. 301, no. 2, pp. 855–874, 2022.

Yuxin Li was born in Chongqing, China,in 1999. She obtained her Bachelor degree in Traffic and Transportation from Chongqing Jiaotong University, Chongqing, China, 2021.

She is currently pursuing a master's degree in Traffic and Transportation (Traffic and Transportation Planning and Management) at Lanzhou Jiaotong University. Her research interests include: train timetabling and rolling stock circulation.